

# Impact ionization threshold energy of trigonal selenium: An ab initio study<sup>1</sup>

A. Darbandi and O. Rubel

**Abstract:** Impact ionization coefficient is a critical parameter that determines the multiplication gain in avalanche photodiodes. The impact ionization coefficient is closely related to the ionization threshold,  $E_{th}$ , which is determined by the band dispersion of the semiconducting material used in detectors. The ionization threshold energy is commonly calculated based on a parabolic band assumption, which provides only a crude approximation. Here we present a first principle study of the ionization threshold energy through an analysis of the electronic structure of trigonal selenium. It is shown that the excess energy of primary charge carriers required to initiate the impact ionization in trigonal selenium can be as low as the band gap,  $E_g$ , which is a sharp contrast to the parabolic band approximation that implies  $E_{th} = 3/2E_g$ . Such a low  $E_{th}$  value is a favourable factor for impact ionization.

PACS Nos.: 71.20.-b, 71.20.Mq, 73.50.Fq.

**Résumé :** Le coefficient d'ionisation par impact est un paramètre critique qui détermine le gain par multiplication dans l'avalanche d'une photodiode. Ce paramètre est très relié au seuil d'ionisation,  $E_{th}$ , qui est déterminé par la dispersion de bande du semi-conducteur utilisé dans le détecteur. L'énergie de seuil d'ionisation est généralement calculée en se basant sur une hypothèse de bande parabolique, ce qui est une approximation grossière. Nous présentons ici une étude à partir de principes premiers pour l'énergie du seuil d'ionisation, via une analyse de la structure électronique du sélénium trigonal. Nous montrons que l'excès d'énergie des porteurs primaires de charge, requise pour initier l'ionisation par impact dans le sélénium trigonal, peut être aussi basse que la séparation (gap) de bande  $E_g$ , ce qui est en contraste marqué avec l'approximation parabolique qui implique  $E_{th} = 3/2E_g$ . Une aussi basse valeur pour  $E_{th}$  favorise l'ionisation par impact. [Traduit par la Rédaction]

## 1. Introduction

Impact ionization and subsequent avalanche multiplication of charge carriers is widely studied in amorphous selenium-based (a-Se) avalanche photosensors, which have found an application in high-sensitivity photosensors for television camera tubes [1]. The favourable combination of photoconducting properties of a-Se with the impact ionization holds a potential for advancement of  $\gamma$ -ray and possibly X-ray detectors for medical imaging [2–6].

The theory of impact ionization in crystalline semiconductors was established through the development of the lucky drift model [7–10]. This model was further extended to amorphous semiconductors taking into account the elastic scattering with a disorder potential [11–14]. In this model, the charge carriers gain excess energy from the external electric field while drifting. Once a charge carrier attains a kinetic energy equal to the ionization threshold energy,  $E_{th}$ , it can ionize the lattice atoms through an inelastic collision and create a new electron–hole pair. Low values of  $E_{th}$  are thus a favourable factor for impact ionization and avalanche multiplication.

The parabolic band approximation is usually applied to estimate the ionization threshold. This approximation yields  $E_{th} = E_g + 1/2E_g$  [15], where  $E_g$  is the semiconductor band gap energy. The additional term  $1/2E_g$  comes from necessity to fulfill conservation of momentum. In ref. 16 it is noted that the threshold energy calculated using the parabolic band approximation leads to an overestimation of the pair-creation energy in a-Se by approximately 2 eV. The contradiction was resolved by eliminating the  $1/2E_g$  component motivated by loosening momentum conservation because of the disordered structure of a-Se [16].

It is widely believed that wave vector  $\mathbf{k}$ , is not a good quantum number in amorphous structures because of the lack of periodic potentials in these materials [17]. However, a more detailed analysis reveals that the dispersion of the extended-state wavefunctions for amorphous and crystalline solids are comparable, however, no periodic function for localized states can be defined because of the presence of disorder [18]. Therefore, the momentum,  $\mathbf{k}$ , may not be a valid quantum number for the localized states in Bloch's solution, but it still applies to the extended states, which are involved in impact ionization, in the amorphous structure [19].

Here we perform a detailed study of the electronic structure of trigonal selenium (t-Se). It is assumed that the obtained results are applicable to the amorphous phase. This assumption is supported by X-ray ultraviolet and inverse photoemission measurements [20–22], which reveal an almost identical density of states in a-Se and t-Se. The study of the neutron inelastic scattering also provides a similar phonon density of states in both a-Se and t-Se [23]. Our analysis suggests that the threshold energy in t-Se is indeed close to  $E_g$ , which is a consequence of its indirect band structure. Therefore, no violation of momentum conservation is required.

## 2. Methods

A necessary condition for the impact ionization to occur is that all initiating and resultant particles should satisfy the energy and momentum conservation requirements

$$E(\mathbf{k}_1, n_1) + E(\mathbf{k}_2, n_2) = E(\mathbf{k}_1', n_1') + E(\mathbf{k}_2', n_2') \quad (1)$$

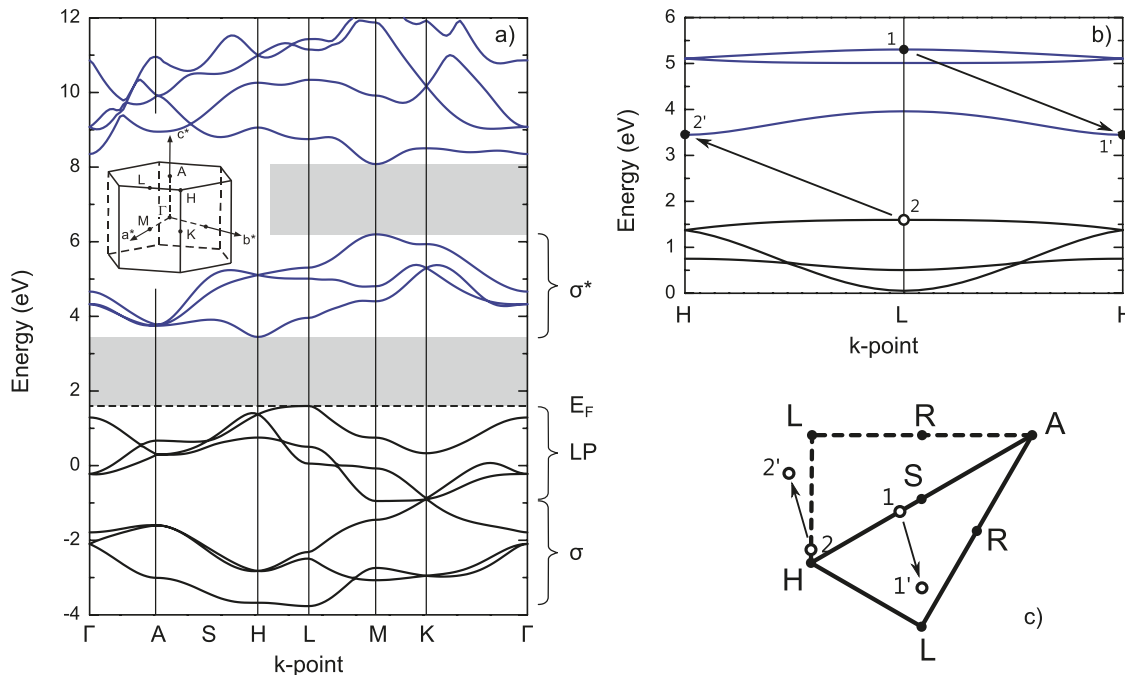
Received 2 November 2012. Accepted 4 January 2013.

A. Darbandi and O. Rubel. Thunder Bay Regional Research Institute, 290 Munro St, Thunder Bay, Ontario, Canada; Lakehead University, 955 Oliver Road, Thunder Bay, Ontario, Canada.

Corresponding author: O. Rubel (e-mail: rubelo@tbh.net).

<sup>1</sup>This paper was presented at the Theory CANADA 7 conference, held 7–9 June 2012 at The University of Lethbridge, Lethbridge, Alberta, Canada.

**Fig. 1.** (a) Band structure of t-Se along high-symmetry points in the Brillouin zone, which is shown in the inset. Bonding,  $\sigma$ ; antibonding,  $\sigma^*$ ; and lone-pair (LP) states are indicated. The shaded areas correspond to the optical gap and the gap between two conduction bands (from bottom to top, respectively). (b) The band structure along the H–L–H segment with four particles involved into the electron ionization event near the threshold. (c) Top view of the Brillouin zone with  $k$ -points involved in the hole ionization event near to the threshold.



$$\mathbf{k}_1 + \mathbf{k}_2 = \mathbf{k}_{1'} + \mathbf{k}_{2'} \quad (2)$$

where  $\mathbf{k}_i$  is the electron wave vector,  $n_i$  is the band index, and  $E(\mathbf{k}_i, n_i)$  is the corresponding energy eigenvalue. The indices 1, 2 and 1', 2' represent the initiating and resultant carriers, respectively. The ionization energy corresponds to the excess energy of the primary carrier, 1.

Further analysis of the ionization threshold for electrons and holes in t-Se requires detailed knowledge of the band structure, which can be obtained self-consistently using density functional theory (DFT) and an equilibrium atomic structure. The structure of t-Se consists of parallel helical chains arranged with a hexagonal symmetry, which can be characterized by two lattice constants,  $a$  and  $c$ , and the diameter of the chain,  $\rho$  [24]. The full structural optimization was performed using the plane-wave method implemented in the ABINIT package [25, 26], generalized gradient approximations [27], and Troullier–Martins pseudopotential [28, 29]. Convergence tests were performed with respect to the  $k$ -mesh density and the plane wave cutoff energy,  $E_{\text{cut}}$ . Convergence was reached at  $E_{\text{cut}} = 25$  Ha (1 Ha = 27.211 385 05(60) eV) and  $4 \times 4 \times 4$  Monkhorst–Pack  $k$ -point mesh [30]. The obtained lattice parameters are  $a = 4.54$  Å,  $c = 5.05$  Å, and  $\rho = 2.0$  Å. The deviation between theoretical and experimental structural parameters did not exceed 6% [31].

The calculated band structure of t-Se is presented in Fig. 1. Trigonal selenium is an indirect semiconductor with the lowest energy transition between L-point in the top of valence band and H-point in the bottom of the conduction band. The DFT energy gap is about 1 eV, which is significantly underestimated with respect to the experimental value of 1.85 eV [32–34]. This inconsistency is attributed to a well-known shortcoming of explicit density-dependent functionals, which tend to underestimate the energy gap [35]. In Fig. 1 and the following analysis, the so-called “scissor operator” (energy offset) was applied to match the theoretical energy gap with its experimental value.

The necessary precursor for impact ionization is a low threshold energy of a primary charge carrier. In the search for the ionization threshold, we sample the entire Brillouin zone using 6400  $k$ -points ( $20 \times 20 \times 16$  mesh). Next, we analyze all possible ionization events by generating combinations of four  $k$ -points that obey (2). For each set of  $k$ -points and the combination of four bands ( $n_1, n_2, n_{1'}, n_{2'}$ ) involved in the impact ionization event, the energy conservation criterion (1) is evaluated using a gaussian approximation for the delta function with the smearing of 50 meV. This approach provides the resolution of approximately 20 meV for the ionization energy, which is sufficient for the purpose of our discussion. The threshold energy is identified as the lowest possible ionization energy that satisfies the conservation rules.

### 3. Results and discussion

The analysis of the electronic structure of t-Se yields an ionization threshold of 1.85 eV for electrons as primary charge carriers. The charge carriers with the lowest ionization energy are located along the H–L–H segment of the Brillouin zone (see Fig. 1b). The resultant carriers 1', 2, and 2' occupy states in the valence band maximum (L-point) and the conduction band minimum (H-point), which ensures the lowest possible ionization energy  $E_{\text{th,e}} = E_g$ , providing a sharp contrast to the parabolic band approximation [15], which predicts  $E_{\text{th}} = 1.5E_g$ .

Results of our calculations suggest that the ionization energy for primary holes amounts to 1.95 eV ( $E_{\text{th,h}} = 1.05E_g$ ), which is slightly greater than that for electrons. The interpretation of this result requires further analysis of the valence band dispersion. For the energy threshold to be equal to the band gap, the resultant carriers 1', 2, and 2' should not have any excess energy, that is, occupy the valence band maximum and the conduction band minimum (L and H points, respectively). In this case, the momentum conservation dictates that the wave vector of the primary carrier,  $\mathbf{k}_1$ , should be either at point H or S (see Fig. 1c). Apparently, the excess energy of holes in H and S points of the lone pair band does

not exceed the band gap (see Fig. 1a), which precludes their participation in the impact ionization. Therefore, the wave vectors of particles participating in the impact ionization of holes near the threshold deviate from these high symmetry points, as shown in Fig. 1c, resulting in a value of ionization energy slightly higher than  $E_g$ , but still lower than  $1.5E_g$ . The low ratio  $E_{th}/E_g \approx 1$  is a consequence of an indirect band structure inherent to t-Se, which is a positive factor for the avalanche gain.

The minimum set of parameters that are involved in the theoretical determination of the impact ionization coefficient in disordered solids is: the ionization threshold,  $E_{th}$ , optical phonon mean free path,  $\lambda_{op}$ , optical phonon energy,  $\hbar\omega$ , and the momentum relaxation mean free path,  $\lambda_m$ , because of scattering with disorder [11]. The field-dependent impact ionization coefficient can be approximated in terms of these parameters as [14]

$$\alpha \approx \frac{2\hbar\omega}{\lambda_m\lambda_{op}eF} \exp\left(-\frac{2\hbar\omega E_{th}}{\lambda_m\lambda_{op}e^2F^2}\right) \quad (3)$$

where  $F$  is the electric field strength. The low disparity between the values of  $E_{th,e}$  and  $E_{th,h}$  suggests similar impact ionization coefficients ( $\alpha$  and  $\beta$ ) for both electrons and holes in t-Se. However, it has been observed experimentally that the avalanche multiplication in polycrystalline t-Se [36] and a-Se [37] is dominated by holes with a ratio of about  $\beta/\alpha \gg 10$  and  $\beta/\alpha \gg 10$ –100, respectively. The dominant avalanche of holes can be interpreted through an analysis of the mean free paths,  $\lambda_{op}$  and  $\lambda_m$ .

It has been observed experimentally that the hole mobility in a-Se is in the range 0.12–0.14 cm<sup>2</sup>V<sup>-1</sup>s<sup>-1</sup>, whereas the corresponding values for electrons are 0.003–0.006 cm<sup>2</sup>V<sup>-1</sup>s<sup>-1</sup> [38, 39]. This indicates a shorter mean free path,  $\lambda_m$ , for electrons than for holes, because the mobility is controlled by scattering with disorder. It has also been shown that the electron – optical phonon interaction is stronger for electrons than for holes [31], which implies a shorter optical mean free path,  $\lambda_{op}$ , for electrons than for holes. Consequently, the greater value of the product  $\lambda_m\lambda_{op}$  in (3) favours the avalanche multiplication of holes, which agrees with experimental observations for both t-Se and a-Se.

#### 4. Conclusion

We calculated the ionization threshold for electrons and holes in t-Se to elucidate the origin of deviation of experimental threshold energies from those predicted by the parabolic band approximation. The calculations were based on the full band structure of t-Se, which was obtained self-consistently in the framework of a density functional theory. The results suggest that the excess energy of a primary carrier required to generate the secondary electron–hole pair in t-Se is approximately equal to the energy gap ( $E_{th} \approx E_g$ ), which is significantly lower than the result predicted by the parabolic band approximation ( $E_{th} = 1.5E_g$ ). Such a low ionization threshold for both electrons and holes in t-Se is attributed to its indirect band structure. This scenario provides an alternative to the violation of conservation of momentum, which was formerly put forward in the literature to explain low  $E_{th}$  values in a-Se.

#### Acknowledgements

Financial support from the Natural Sciences and Engineering Research Council of Canada under a Discovery Grants Program “Microscopic theory of high-field transport in disordered semiconductors” and Thunder Bay Community Economic and Development Commission is highly acknowledged.

#### References

1. K. Tanioka, J. Yamazaki, K. Shidara, K. Taketoshi, T. Kawamura, S. Ishioka, and Y. Takasaki. IEEE Electr. Device. L, **8**, 392 (1987). doi:10.1109/EDL.1987.26671.
2. H.M. Rougeot and G.E. Possin. United States Patent p. 5198673. 1993.
3. W. Zhao, D. Li, A. Reznik, B. Lui, D. Hunt, K. Tanioka, and J. Rowlands. Proc. SPIE **5745**, 352 (2005). doi:10.1117/12.597295.
4. A. Reznik, B. Lui, and J.A. Rowlands. Technol. Cancer Res. Treat, **4**, 61 (2005). PMID:15649089.
5. A. Reznik, S.D. Baranovskii, O. Rubel, K. Jandieri, S. Kasap, Y. Ohkawa, M. Kubota, K. Tanioka, and J. Rowlands. J. Non-Cryst. Solids, **354**, 2691 (2008). doi:10.1016/j.jnoncrysol.2007.09.058.
6. S. Kasap, J.B. Frey, G. Belev, O. Tousignant, H. Mani, L. Laperriere, A. Reznik, and J.A. Rowlands. Phys. Status Solidi B, **246**, 1794 (2009). doi:10.1002/pssb.200982007.
7. P.A. Wolff. Phys. Rev. **95**, 1415 (1954). doi:10.1103/PhysRev.95.1415.
8. W. Shockley. Solid-State Electron. **2**, 35 (1961). doi:10.1016/0038-1101(61)90054-5.
9. G.A. Baraff. Phys. Rev. **128**, 2507 (1962). doi:10.1103/PhysRev.128.2507.
10. B.K. Ridley. J. Phys. C: Solid State Phys. **16**, 3373 (1983). doi:10.1088/0022-3719/16/17/020.
11. O. Rubel, S.D. Baranovskii, I.P. Zvyagin, P. Thomas, and S.O. Kasap. Phys. Status Solidi C, **1**, 1186 (2004). doi:10.1002/pssc.200304319.
12. S. Kasap, J.A. Rowlands, S.D. Baranovskii, and K. Tanioka. J. Appl. Phys. **96**, 2037 (2004). doi:10.1063/1.1763986.
13. K. Jandieri, O. Rubel, S.D. Baranovskii, A. Reznik, J.A. Rowlands, and S.O. Kasap. J. Mater. Sci: Mater. Electron. **20**, 221 (2009). doi:10.1007/s10854-007-9549-1.
14. O. Rubel, A. Potvin, and D. Laughton. J. Phys. Condens. Matter, **23**, 055802 (2011). doi:10.1088/0953-8984/23/5/055802. PMID:21406915.
15. C.L. Anderson and C.R. Crowell. Phys. Rev. B, **5**, 2267 (1972). doi:10.1103/PhysRevB.5.2267.
16. W. Que and J.A. Rowlands. Phys. Rev. B, **51**, 10500 (1995). doi:10.1103/PhysRevB.51.10500.
17. O. Madelung. Introduction to solid-state theory. Springer. 1995. p. 443.
18. R.A. Street. Hydrogenated amorphous silicon. Cambridge University Press. 2005. Ch. 1.
19. J. Singh and K. Shimakawa. Advances in amorphous semiconductors. CRC Press. 2003.
20. N.J. Shevchik, J. Tejada, M. Cardona, and D.W. Langer. Solid State Commun. **12**, 1285 (1973). doi:10.1016/0038-1098(73)90866-1.
21. N.J. Shevchik, M. Cardona, and J. Tejada. Phys. Rev. B, **8**, 2833 (1973). doi:10.1103/PhysRevB.8.2833.
22. I. Ono, P.C. Grekos, T. Kouchi, M. Nakatake, M. Tamura, S. Hosokawa, H. Namatame, and M. Taniguchi. J. Phys.: Condens. Matter, **8**, 7249 (1996). doi:10.1088/0953-8984/8/39/004.
23. F. Gompf. J. Phys. Chem. Solids, **42**, 539 (1981). doi:10.1016/0022-3697(81)90037-8.
24. P. Cherin and P. Unger. Inorg. Chem. **6**, 1589 (1967). doi:10.1021/ic50054a037.
25. X. Gonze, G.-M. Rignanese, M. Verstraete, J.-M. Beuken, Y. Pouillon, R. Caracas, F. Jollet, M. Torrent, G. Zerah, M. Mikami, et al. Zeit. Kristallogr. **220**, 558 (2005). doi:10.1524/zkri.220.5.558.65066.
26. X. Gonze, J.-M. Beuken, R. Caracas, F. Detraux, M. Fuchs, G.-M. Rignanese, L. Sindic, M. Verstraete, G. Zerah, F. Jollet, et al. Comp. Mater. Sci. **25**, 478 (2002). doi:10.1016/S0927-0256(02)00325-7.
27. J.P. Perdew, K. Burke, and M. Ernzerhof. Phys. Rev. Lett. **77**, 3865 (1996). doi:10.1103/PhysRevLett.77.3865. PMID:10062328.
28. N. Troullier and J.L. Martins. Phys. Rev. B, **43**, 1993 (1991). doi:10.1103/PhysRevB.43.1993.
29. M. Fuchs and M. Scheffler. Comp. Phys. Comm. **119**, 67 (1999). doi:10.1016/S0010-4655(98)00201-X.
30. H.J. Monkhorst and J.D. Pack. Phys. Rev. B, **13**, 5188 (1976). doi:10.1103/PhysRevB.13.5188.
31. A. Darbandi and O. Rubel. J. Non-Cryst. Solids, **358**, 2434 (2012). doi:10.1016/j.jnoncrysol.2011.11.032.
32. R. Fischer. Phys. Rev. B, **5**, 3087 (1972). doi:10.1103/PhysRevB.5.3087.
33. B. Moreth. Phys. Rev. Lett. **42**, 264 (1979). doi:10.1103/PhysRevLett.42.264.
34. M. Takumi, Y. Tsujioka, N. Hirai, K. Yamamoto, and K. Nagata. J. Phys.: Conf. Ser. **215**, 012049 (2010). doi:10.1088/1742-6596/215/1/012049.
35. J.P. Perdew. Int. J. Quantum Chem. **28**, 497 (1985).
36. H.P.D. Lanyon and R.E. Richardson. Phys. Status Solidi A, **7**, 421 (1971). doi:10.1002/pssa.2210070215.
37. K. Tsuji, Y. Takasaki, T. Hirai, and K. Taketoshi. J. Non-Cryst. Solids, **114**, 94 (1989). doi:10.1016/0022-3093(89)90079-3.
38. G. Juska and K. Arlauskas. Phys. Status Solidi A, **59**, 389 (1980). doi:10.1002/pssa.2210590151.
39. S. Kasap and J. Rowlands. J Mater Sci.: Mater Electron. **11**, 179 (2000). doi:10.1023/A:1008993813689.